SWIFT-XRT-CALDB-04
Release Date: April 21st, 2008
Prepared by: Claudio Pagani, David Morris (PSU)
Date Revised: 25 April 2008
Revision 8.0
Revised by: Claudio Pagani (PSU)
Pages Changed: all

SWIFT XRT CALDB REV 8.0 RELEASE NOTE
SWIFT-XRT-CALDB-04: Gain

1. COMPONENT FILES

FILENAME	VALID DATE	RELEASE DATE	VERSION
swxpcgain20010101v003.fits	1-Jan-2001	15-Oct-2004	003
swxpdgain20010101v003.fits	1-Jan-2001	15-Oct-2004	003
swxwtgain20010101v003.fits	1-Jan-2001	15-Oct-2004	003
swxpcgain20010101v004.fits	1-Jan-2001	10-Jan-2005	004
swxpdgain20010101v004.fits	1-Jan-2001	10-Jan-2005	004
swxwtgain20010101v004.fits	1-Jan-2001	10-Jan-2005	004
swxpcgain20010101v005.fits	1-Sep-2005	12-Oct-2005	005
swxpdgain20010101v005.fits	1-Sep-2005	12-Oct-2005	005
swxwtgain20010101v005.fits	1-Sep-2005	12-Oct-2005	005
swxpcgain20010101v006.fits	1-Sep-2005	1-Dec-2005	006
swxpdgain20010101v006.fits	1-Sep-2005	1-Dec-2005	006
swxwtgain20010101v006.fits	1-Sep-2005	1-Dec-2005	006
swxpcgains0_20010101v007.fits	1-Sep-2005	30-Jul-2007	007
swxpcgains6_20010101v007.fits	1-Sep-2005	30-Jul-2007	007
swxpdgains0_20010101v007.fits	1-Sep-2005	30-Jul-2007	007
swxwtgains0_20010101v007.fits	1-Sep-2005	30-Jul-2007	007
swxwtgains6_20010101v007.fits	1-Sep-2005	30-Jul-2007	007
swxwtgains0_20010101v008.fits	1-Sep-2005	21-Apr-2008	008
swxwtgains6_20010101v008.fits	1-Sep-2005	21-Apr-2008	008

Tab 1: Component files.

2. SCOPE OF DOCUMENT

This document contains a description of the gain calibration analysis performed at Penn State and Leicester University to produce the gain calibration products for the XRT Calibration Database.

3. CHANGES IN GAIN RELEASE VERSION 08

Energy Offset in Windowed Timing Gain files

The Windowed Timing Gain files have been updated with the introduction of an energy offset of 17.6 eV. The change was required to account for the observed systematic errors in WT mode spectra around the Oxygen, Silicon and Gold edges (for more details, please see Sec. 8, the current Release Note on Response matrices and ancillary Response files and also Godet et al. 2007, SPIE, 6686).

Previous CALDB releases included ad-hoc corrections in the WT ancillary files (versions 8, 9 and 10) to account for the observed absorption-like features. Further investigation, with the comparison of spectral lines of calibration sources as CasA and 1ES 0102-72.2 observed in Photon Counting and Windowed Timing showed these features to be caused by an energy scale offset of 17.6 eV between the modes (see Figures 1, 2). Thanks to the introduction of the observed energy offset in the WT gain files the ad-hoc corrections around the oxygen edge are no longer necessary. Updated versions of the ancillary response files to be used in combination with the new WT gain files are included in this release.

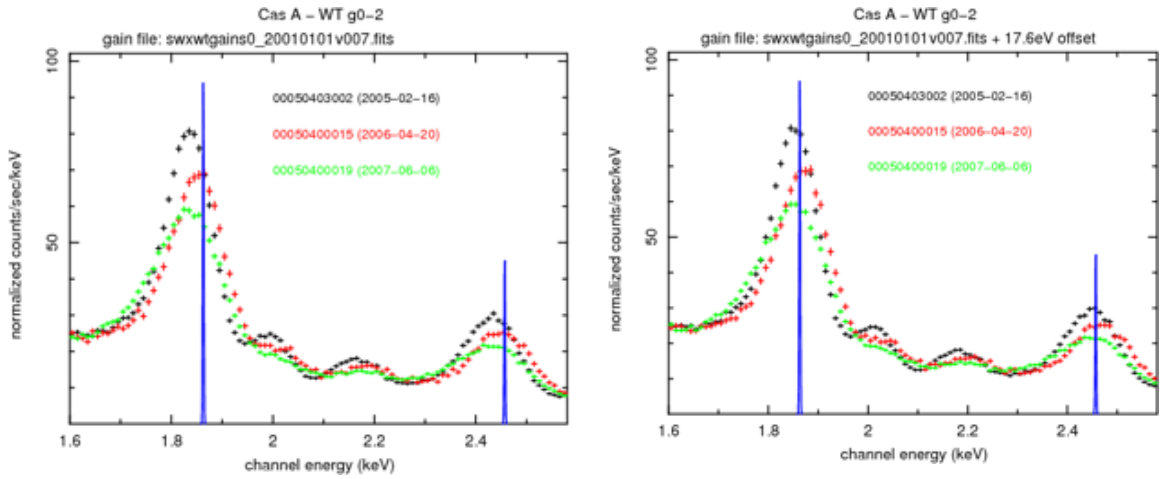

Fig. 1: On the left, the Cas A Windowed Timing spectral fit using previous versions of the gain file. On the right, the spectral fit obtained using the gain with a 17.6 eV energy offset. The blue lines indicate the spectral lines true energy values.

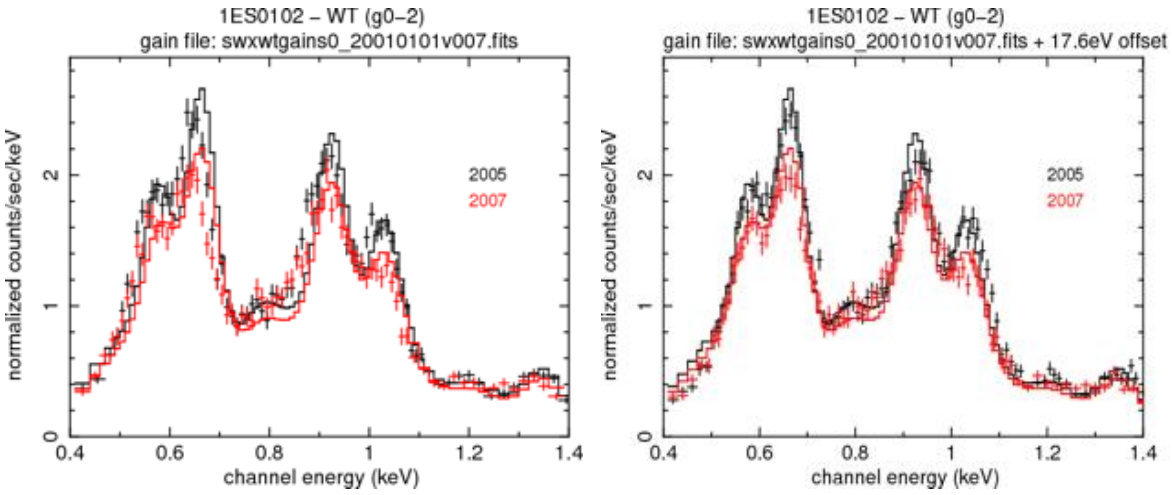

Fig. 2: The comparison of the Windowed Timing spectral fits of 1ES 0102-72.2 using the previous version of the gain file, on the left, and the spectral fits using the gain file with the 17.6 eV energy offset applied, on the right.

4. SCIENTIFIC IMPACT OF THIS UPDATE

The accuracy of XRT spectral feature energy centroids in Windowed Timing data should be significantly improved thanks to the energy offset introduced in the updated WT files.

5. EXPECTED UPDATES

Radiation damage during the orbital lifetime of Swift is degrading the XRT CCD charge transfer efficiency (CTE) mostly through the production of charge traps. The gain and CTE coefficients are continuously monitored using the ^{55}Fe calibration sources mounted at the 4 corners of the detector for in-flight calibration (see Sec. 7). The coefficients are updated in the gain files on a regular base.

6. DEFINITION AND DERIVATION OF THE GAIN FILES COEFFICIENTS

The gain in the CALDB product is specified as:

$$PI = ((PHA*(GC0 + x*GC1 + y*GC2) + GC3 + x*GC4 + y*GC5)/G),$$

where PI is the pulse invariant bin, PHA is the pulse height amplitude, x/y is the detector x/y coordinate of the event, G is a global PHA to PI gain factor and the 6 coefficients are as follows:

GC0: multiplicative DN to PHA gain factor
GC1: multiplicative serial CTI correction factor
GC2: multiplicative parallel CTI correction factor
GC3: additive gain correction in eV

GC4: additive serial CTI correction
GC5: additive parallel CTI correction

The gain coefficients are functions of time and temperature. We currently set GC3=GC4=GC5=0 and G=10, so that the PHA to PI conversion is:

$$PI = (PHA/G)*(GC0 + x*GC1 + y*GC2),$$

The Charge Transfer Efficiency measures the amount of charge lost in the transfer from the i^{th} to the $(i+1)^{th}$ pixel, such that $Q_{i+1}=Q_i*CTE$. After N transfers the remaining charge is

$$Q_N=Q_0*(CTE)^N,$$

where Q_0 is the initial charge. Defining CTE_p and CTE_s the Parallel and Serial Charge Transfer Efficiency respectively the final charge value on reaching the output amplifier is therefore:

$$Q=Q_0*(CTE_p)^{Np}*(CTE_s)^{Ns},$$

for charge transferred through N_p pixels in the parallel direction and N_s pixels in the serial direction. Including a term for the charge lost in the CCD22 frame-store section, the above equation becomes:

$$Q=Q_0*(CTE_{Pf})^{Yfs}*(CTE_{pi})^{x}*(CTE_s)^{y},$$

Where (x,y) are the pixel detector coordinates and Y_{fs} = 600 is the number of rows in the frame store section, CTE_{pf} is the CTE during the frame transfer and CTE_{pi} is the image CTE measured during the frame readout. Inverting the equation to estimate the original charge from the measured charge and working in terms of the Charge Transfer Inefficiency CTI=1-CTE, (which is typically $\sim 10^{-5}$, therefore allowing the use of the small value approximations) we obtain:

$$Q_0 = Q*(1- CTI_{Pf})^{-Yfs} (1-CTI_{pi})^{-y}*(1-CTI_s)^{-x}$$

$$\approx Q*(1+ Y_{fs}*CTI_{Pf})*(1+y*CTI_{pi})*(1+x*CTI_s)$$

$$\approx Q*(1+ Y_{fs}*CTI_{Pf})*(1+x*CTI_s+y*CTI_{pi})$$

Comparing the above equation with the CALDB gain file definition we obtain that the GC0 coefficient is the gain value, including both the amplifier gain and the degradation in that gain caused by charge loss during the frame-store transfer, and

$$GC1=GC0*CTI_s$$
$$GC2=GC0*CTI_{pi}$$

The gain and CTI coefficients are monitored using the four calibration corner sources (see Section 8). Relating the coefficients to measured values we obtain:

- *GC0* is the measured gain factor for ^{55}Fe events from corner source cs3, the one nearest the output amplifier.
- *GC1* is the product of the gain and the *serial CTI*, measured using corner source pairs *cs1* and *cs2* or *cs3* and *cs4*
- *GC2* is the product of the gain and the *parallel CTI*, measured using corner source pairs *cs1* and *cs3* or *cs2* and *cs4*

7. GAIN

Introduction

The XRT CCD has 4 ^{55}Fe calibration sources mounted at the corners of the detector that continuously illuminate the non-imaging area of the CCD for in-flight calibration and monitoring. The decay of ^{55}Fe to ^{55}Mn in the calibration sources produces a doublet line (Mn K□) at 5.88 and 5.899 keV and a weaker, singlet line (Mn K□) at 6.49 keV. In addition to the sources mounted on the CCD, a ^{55}Fe source mounted on the back of the XRT focal plane camera door illuminates the focal plane while the door is in the closed position (that is, blocking the optical path). The regions of the detector illuminated by each source can be clearly seen in the figure below.

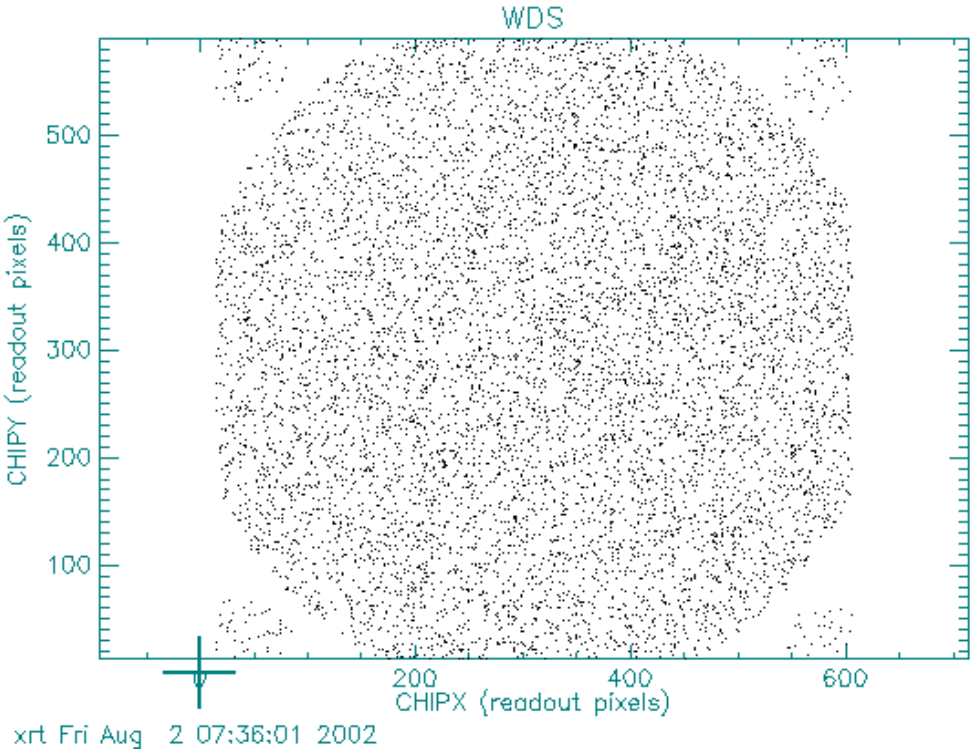

Fig. 3: XRT CCD detector illuminated by the calibration sources.

We will henceforth define the XRT corner source configuration as follows:

DetX>
CS1 CS2
^
DetY
CS3 CS4
SERIAL REG
amp/

The XRT Photon Counting data transmitted to the ground at the start of the mission consisted of a 475x475 pixels window (the entire CCD area is 600x600 pixels) to reduce data volume to satisfy *Swift*'s telemetry requirements. The transmitted window was increased to 500x500 pixels starting on October 2005 to include more corner source events to produce better statistics to monitor the gain and the CTI evolution.

Events collected from the corner sources are merged on a monthly basis. A preliminary analysis to identify traps caused by proton damage of the CCD was performed and columns with charge traps that can cause energy shifts and line widening are excluded. The centroids of the Mn k-□spectral line are used to evaluate gain values and serial and parallel CTI coefficients. In particular, we used the spectral data from the corner source # 3 (cs3) at the bottom left of the detector (the source closest to the amplifier) to monitor the gain evolution.

Gain Analysis

In the following figure we show the gain coefficients from the analysis of the four corner sources since the start of the mission (cs3 is in blue).

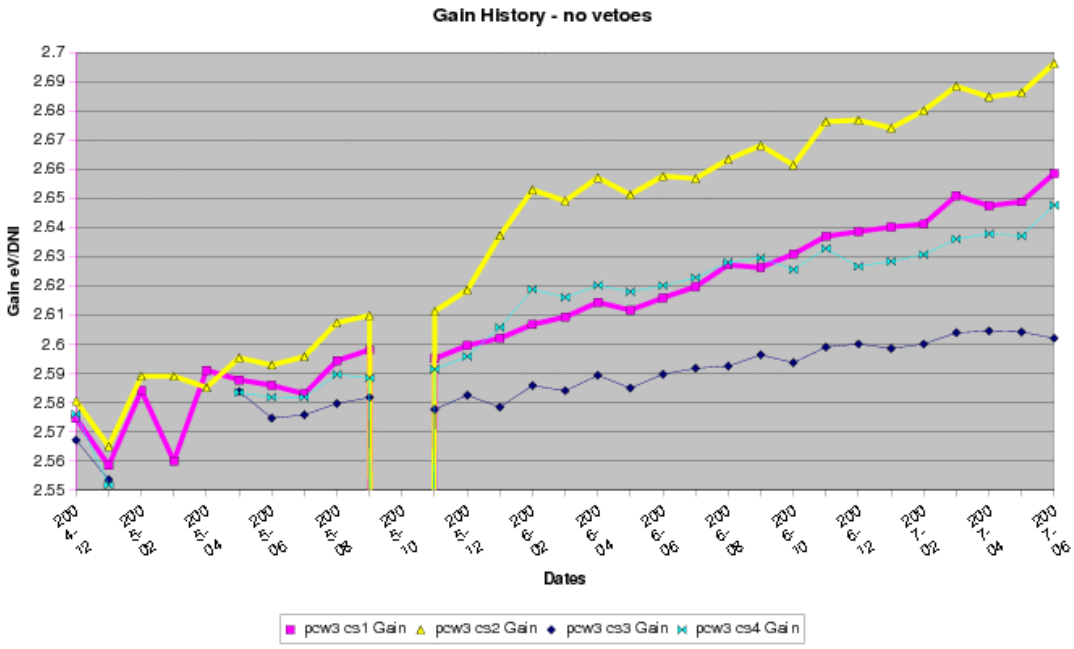

Fig. 4: Gain factors calculated from the energy line fit of the four calibration corner sources. The size of the Photon Counting window transmitted on the ground has been increased to 500x500 pixels starting on October 2005 to include a higher number of corner sources events to obtain good statistics for a detailed monitoring of gain and CTI changes. The gain value used in the CALDB is from the corner source #3 (cs3) data, the nearest to the amplifier.

The following gain coefficients, obtained from a best linear fit of the measured cs3 gain values were included in the CALDB file *swxpcgains0_20010101v011.fits*:

DATE	Gain
2005-09-01:00:00	2.5795
2005-11-01:00:00	2.5819
2005-12-01:00:00	2.5831
2006-01-01:00:00	2.5843
2006-05-01:00:00	2.5891
2006-08-01:00:00	2.5927
2006-12-01:00:00	2.5975
2007-01-01:00:00	2.5987
2007-03-01:00:00	2.6011
2007-06-01:00:00	2.6047

Tab 2: Gain factors derived from the calibration corner sources analysis.

The CALDB files contain gain values for CCD temperatures of -100C, -65C and -48C. The corner source events are collected at all operating CCD temperatures, which can vary from -50C to -75C depending on the efficiency of the passive cooling. The statistics in our dataset are too low to discriminate between corner source events collected at different CCD temperatures, and we considered the calculated gain values to be representative of the gain coefficients at -65C. The gain coefficients at -100C and -48C have been calculated applying the 0.00117eV/DN/^{o}C extrapolation discussed in detail in Section 9.

CTI Analysis:

XRT observations collected after October 2005 are transmitted to the ground with a larger 500x500 pixels window to include a higher number of events from the corner sources. Gaussian centroids for each corner source line are recorded to evaluate serial and parallel CTI evolution. Bad columns affected by traps are excluded from the analysis. The measured serial and parallel CTI values are shown in the figure below. The CTI values in the tables below have been appended in the current release of the CALDB gain file (coefficients GC1 and GC2, see definitions in Section 6).

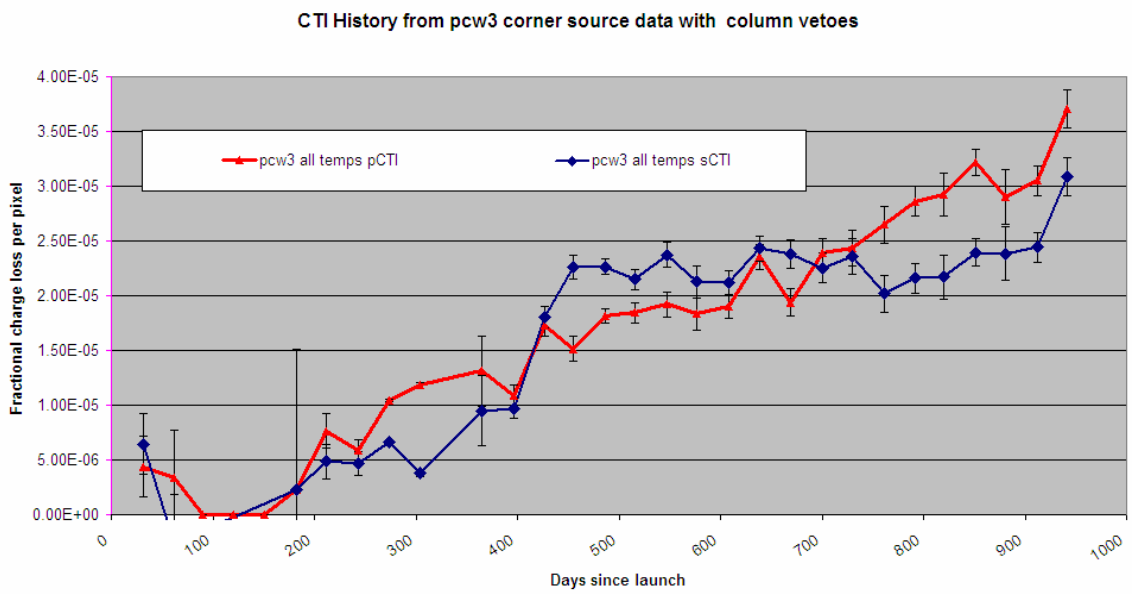

Fig. 5: Serial (in blue) and parallel (in red) CTI coefficients from corner source data. Columns with evidence of traps have been excluded from the analysis.

Table of the Serial CTI, GC1 coefficients in the CALDB file (release version 7)

DATE	$GC1_{-48C}$	$GC1_{-65C}$	$GC1_{-100C}$
2005-09-01:00:00	1.949680E-05	1.935000E-05	1.903500E-05
2005-11-01:00:00	2.464800E-05	2.446788E-05	2.407920E-05
2005-12-01:00:00	2.519400E-05	2.503024E-05	2.462229E-05

2006-01-01:00:00	4.680000E-05	4.651740E-05	4.575600E-05
2006-05-01:00:00	6.183330E-05	6.136166E-05	6.036390E-05
2006-08-01:00:00	6.347160E-05	6.300261E-05	6.198930E-05
2006-12-01:00:00	5.286340E-05	5.246950E-05	5.161100E-05
2007-01-01:00:00	5.654880E-05	5.613192E-05	5.523120E-05
2007-03-01:00:00	6.290400E-05	6.242640E-05	6.141600E-05
2007-06-01:00:00	7.074000E-05	7.032690E-05	6.917400E-05

Tab 3: Serial CTI coefficients from the calibration corner sources.

Table of Parallel CTI, GC2 coefficients in the CALDB file (release version 7)

DATE	**$GC2_{-48C}$**	**$GC2_{-65C}$**	**$GC2_{-100C}$**
8.335040E-05	2.859531E-05	2.838000E-05	2.791800E-05
8.335040E-05	3.406000E-05	3.381110E-05	3.327400E-05
8.335040E-05	2.834000E-05	2.815579E-05	2.769690E-05
8.335040E-05	4.498000E-05	4.470839E-05	4.397660E-05
8.335040E-05	5.009280E-05	4.971072E-05	4.890240E-05
8.335040E-05	6.138200E-05	6.092845E-05	5.994850E-05
8.335040E-05	6.935050E-05	6.883375E-05	6.770750E-05
8.335040E-05	7.487480E-05	7.432282E-05	7.313020E-05
8.335040E-05	8.439620E-05	8.375543E-05	8.239981E-05
8.335040E-05	8.383999E-05	8.335040E-05	8.1984000E-05

Tab 4: Parallel CTI coefficients from the calibration corner sources.

Charge Traps

It is noted that significant charge traps exist in certain columns (as indicated within the document text) of the XRT CCD which may cause the local effective gain to be markedly different from that described by the global gain/CTI coefficients contained in the released gain calibration files. The form of the Calibration Database does not currently allow for precise correction for such traps in the XRT standard processing tools (*xrtpipeline*); the XRT team is presently developing software and CALDB products that will be distributed in future software and CALDB releases that will correct for charge traps.

8. CHANGES IN RELEASE VERSION 7

Substrate Voltage dependent gain

The loss of the CCD active cooling system shortly after launch has forced the instrument to rely on the passive cooling provided by the radiator to operate the detector in the -75C to -50C temperature range. The main effect is a significant level of dark current and CCD noise at low energies with an increasing number of hot and “flickering” pixels at

higher temperatures. The XRT camera has also suffered damage caused by a micrometeoroid impact on 27 May 2005, resulting in the appearance of new hot pixels and hot columns that are now masked on board.

The XRT team has planned a substrate voltage (SSV) change from 0 V to 6 V to reduce the background noise. Observations of Cas A and the Crab at SSV = 6 have shown reduction in the Quantum Efficiency of the order of 10% at 6 keV (Godet *et al.* 2007) and an increase of about 5% in the gain due to the change in the gain of the output FET.

The new CALDB release (20070709) includes two versions of the gain files for Photon Counting (*swxpcgains0_20010101v007.fits* and *swxpcgains6_20010101v007.fits*) and Windowed Timing *(swxwtgains0_20010101v007.fits* & *swxwtgains6_20010101v007.fits*) mode to be used for observations taken at the two SSV values of 0 V and 6 V. The updated *Swift* software (version 2.7.1) will perform a query for the gain file to be used depending on the substrate voltage settings.

Post-Substrate Voltage change Gain

The Substrate Voltage (SSV) increase will cause a gain change. The analysis of the first set of calibration observations of Cas A performed on September 2005 with SSV = 6V has shown a change in the gain by a factor of 1.05 from values from SSV = 0V. An extensive calibration campaign will be performed after the definitive SSV change to characterize the gain change for Photon Counting and Windowed Timing observations. The following gain values are included in the current CALDB release in the files *swxpcgains6_20010101v007.fits* and *swxwtgains6_20010101v007.fits*

DATE	$GC0_{-48}$	$GC0_{-65C}$	$GC0_{-100C}$
2007-07-01:00:00	2.756	2.735	2.690

Tab 5: Gain values at SSV=6V.

Windowed Timing gain offset and spectral fits residuals

The version 7 of the gain files used in combination with the version 10 of RMF and ARF presents a known systematic error for observations taken in Windowed Timing mode around the Oxygen, Silicon and Gold edges. The cause of this error is presently not fully understood and an investigation is ongoing. Spectral line analysis of calibration observations of CasA and 1ES 0102-72.2 showed an offset of 17.6 keV between Photon Counting and Windowed Timing Gaussian centroids fits.
We performed spectral fits of deep observations of Mrk421 and the Crab taken with SSV=0 V to characterize the residuals. Fig. 6 shows the best spectral fit of the Mkn421 observations obtained with the WT gain file version 6 (labeled “CALDB”, in black in the plot) and with version 7 (“new gain”, in red).

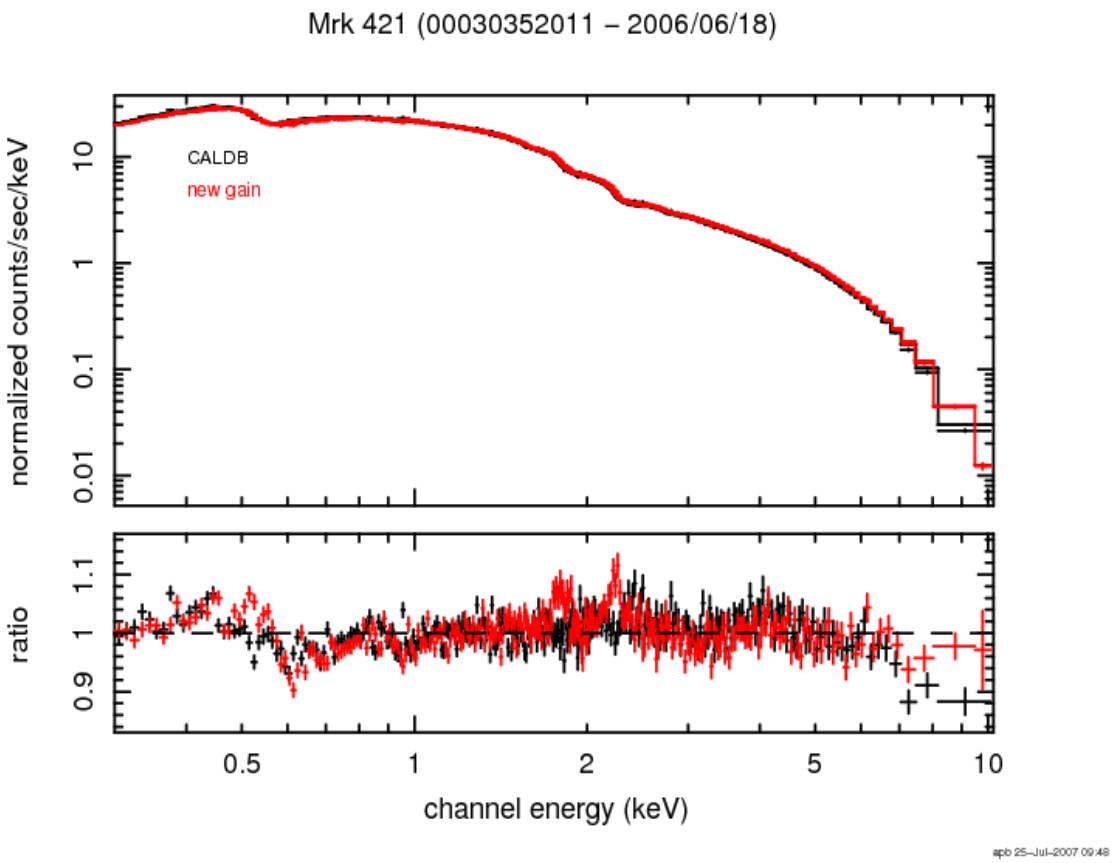

Fig. 6: Best spectral fit of the Mkn 421 WT spectrum using version 6 and version 7 of the CALDB gain files.

We recommend the following corrections to the WT data when using the gain file version 7 in combination with the RMF/ARF release version 10 (for data collected with SSV=0):

Energy	**Residuals (%)**
Si (1.8 keV)	7%
Au (2.25 keV)	10%
O (0.61 keV)	8%

Tab 5: Corrections to the WT spectra for the version 7 of the gain files.

Calibration observations of Mrk421 are planned to characterize these residuals for data collected with the SSV raised to 6 V.

9. CHANGES IN RELEASE VERSION 6

CTI coefficients update, On-Orbit Analysis from September 05 corner sources data

During the first 9 months of the mission, data from the corner sources was unavailable

due to telemetry bandwidth constraints. In September 2005, corner source data was collected which was then used to perform an updated CTI analysis.

Using the nomenclature and method defined above, we find Gaussian centroids for each individual corner source as shown below; 1-sigma Gaussian line width (FWHM/2.35) shown in parentheses and estimated errors:

CS1: 2280 +/- 1 (26.3 +/- 1) DN
CS2: 2272 +/- 1 (27.4 +/- 1) DN
CS3: 2264 +/- 1 (29.1 +/- 1) DN
CS4: 2253 +/- 1 (29.9 +/- 1) DN

yielding CTI measures of (estimated errors):

parallel (1-3) : 1.3×10^{-5} +/- 2×10^{-6}
parallel (2-4) : 1.5×10^{-5} +/- 2×10^{-6}
serial (3-4) : 6.5×10^{-6} +/- 2×10^{-6}

Using this updated analysis, a new set of CTI coefficients has been appended to the Gain CALDB file which will be used to calibrate data collected after September 1, 2005:

serial CTI: 6.5×10^{-6}
parallel CTI: 1.4×10^{-5} (the average across the detector)

Data taken previously to September 1, 2005 will continue to be calibrated using the CTI coefficients defined earlier in the document, which remain in the CALDB gain file to be applied to data collected early in the mission as appropriate.

10. CHANGES IN RELEASE VERSION 5

Temperature Dependent Gain Calibration Factor Analysis

The Gain Calibration CALDB product format has been changed to specify the gain as a function of XRT CCD temperature. The gain is now specified at 3 different XRT CCD temperatures, -100C, -65C and -48C. To determine the actual gain factor to use for a particular XRT data frame, the *xrtpipeline* performs a linear interpolation between the gain factors at each of the 3 specified temperatures to match the temperature of the data frame.

XRT gain calibration is performed in orbit using the well defined lines of the Cassiopeia A supernova remnant (Holt et al 1994, PASJ, 46, L151). It was noted soon after first light that the warmer operating temperature regime caused a change in the XRT gain of ~2%. Further analysis showed that the function of gain with temperature can be fit well by a simple linear relationship. Taking advantage of the wide range of temperatures at which

data have been collected on Cas A together with measurements of the gain at -100^{o}C from ground testing, the XRT gain factor as a function of temperature has been derived. Each of the three XRT observing modes has been calibrated independently, though all are expected to yield similar results. Table 1 shows the dates and XRT CCD temperature ranges of observations used in the gain calibration analysis.

The observations have been separated by CCD temperature, grouping the frames into one degree bins from -46C to -64C. Once each one-degree wide bin of frames had been collected, the resulting spectrum was grouped to have at least 20 counts per PI bin and then analyzed using the XSPECv11 software package to simultaneously fit all lines defined in Holt et. al. using a power-law model plus 14 Gaussian lines.

Once a best fit power law plus multiple Gaussian model was fit to each 1-degree wide data set, a linear fit of known line energy to observed digital number(DN) value was performed to determine the individual gain factor for the dataset at each temperature bin. To minimize the effect of the weaker, more crowded lines in the fit, the fit was performed iteratively, removing the 3-sigma outliers after each successive fit and refitting the remaining lines. Once a gain factor had been determined in this way for each of the 1-degree data sets, a linear function was then fit to the gain factors versus temperature. The fit of gain factor to temperature is weighted by the inverse of the uncertainty in each of the individual gain factors (as defined by the standard deviation of the data in each bin) and is performed iteratively, removing 3-sigma outliers.

Observation Date	**Min CCD_T (C)**	**Max CCD_T (C)**
2004-346	-65	-49
2004-347	-55	-48
2004-358	-64	-47
2005-034	-57	-47
2005-035	-58	-47
2005-047	-65	-51
2005-048	-62	-58

Tab 6: Observation dates and minimum/maximum XRT CCD temperature during the observations of Cassiopeia A data used to calibrate the *Swift* XRT gain in orbit.

This fitting technique produces a temperature dependent correction to the gain factor of 0.00117 eV/DN/^{o}C. If we extrapolate this function backwards from the fitted data to the ground calibration temperature of -100^{o}C, we see that this fit yields a slightly larger value for the gain at -100^{o}C than the ground calibration value of 2.529 eV/DN (the extrapolated value is 2.537). If we assume that the gain truly varies as a linear function across the entire temperature range -100^{o}C to -50^{o}C, then we may recompute our fit including the ground calibration value of the gain at -100^{o}C into our dataset. If we do this and refit the data as described before, the function of the gain factor with temperature becomes (see the figure below) 0.00138 eV/DN/^{o}C. Because we do not have evidence whether the gain does indeed vary linearly with temperature from -100^{o} to -50^{o}C, we have chosen to use the value of 0.00117eV/DN/^{o}C to modify the Gain CALDB file as determined from on orbit data at operational temperatures.

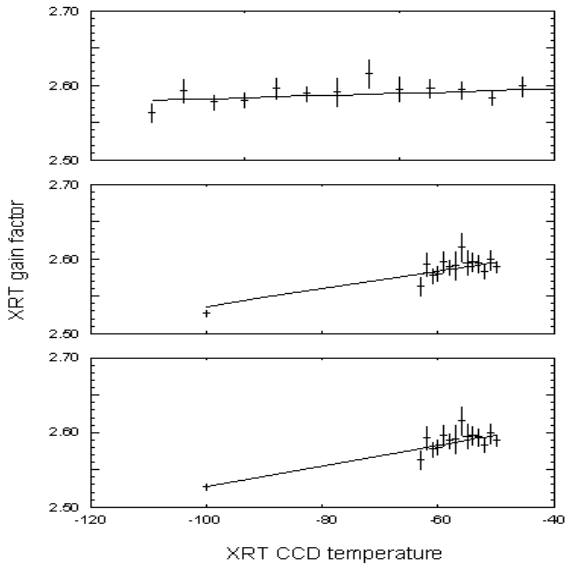

Fig. 7: Fit of XRT gain factor versus XRT CCD temperature. The upper panel shows the fit performed only to the data collected in orbit on Cassiopeia A where the calculated gain correction value is 0.00117 eV/DN/^{o}C. The middle panel is the on-orbit fit extrapolated to the temperature at which ground calibration data was collected, -100^{o}C. The point plotted at -100^{o}C is the gain value determined during ground calibration of 2.529 eV/DN. The lower panel shows the result of fitting for the gain versus temperature factor including all on-orbit data and the ground calibration data collected at -100^{o}C. The gain versus temperature correction factor using all data is 0.00138 ev/DN/^{o}C.

11. CHANGES IN RELEASE VERSION 4

The analysis of observations of the Cassiopeia A supernova remnant (Holt et al 1994, PASJ, 46, L151) taken after first light showed a small change in the gain offset coefficient (coefficient GC3 in the gain file). The gain files have been updated in January 2005 to correct for the measured gain offset change.

12. RELEASE VERSION 3

Panter Gain Calibration

The original gain calibration for the XRT in all modes was determined from data collected at the Panter X-ray calibration facility during Sept-Oct 2002 (with CCD temperature of –100 C). The nominal gain factor in each mode has been determined by performing a linear fit of digital number (DN) to eV of discrete line data collected at energies of 1.49 keV (Al Kα) 4.51keV (Ti Kα), 6.4 keV (Fe Kα) and 8.05 keV (Cu Kα). Data at 0.28 keV (C Kα) were found to be contaminated by background and hence were not used in the calibration. Plots of the gain linearity (in DN vs energy for each mode) are displayed below together with the associated residual of the linear fit to the gain in each mode.

As the current format of the gain Calibration Database file does not support a polynomial description of the gain function, we have chosen to perform the gain calibration using the higher energy values, leaving the slight discrepancy at lower energies to be corrected in later versions of the ground/in-flight calibration. The nominal gain values determined as described above for each mode for the Panter calibration data are:

low rate photodiode: 2.75 eV/DN
photon counting: 2.529 eV/DN
windowed timing: 2.529 eV/DN

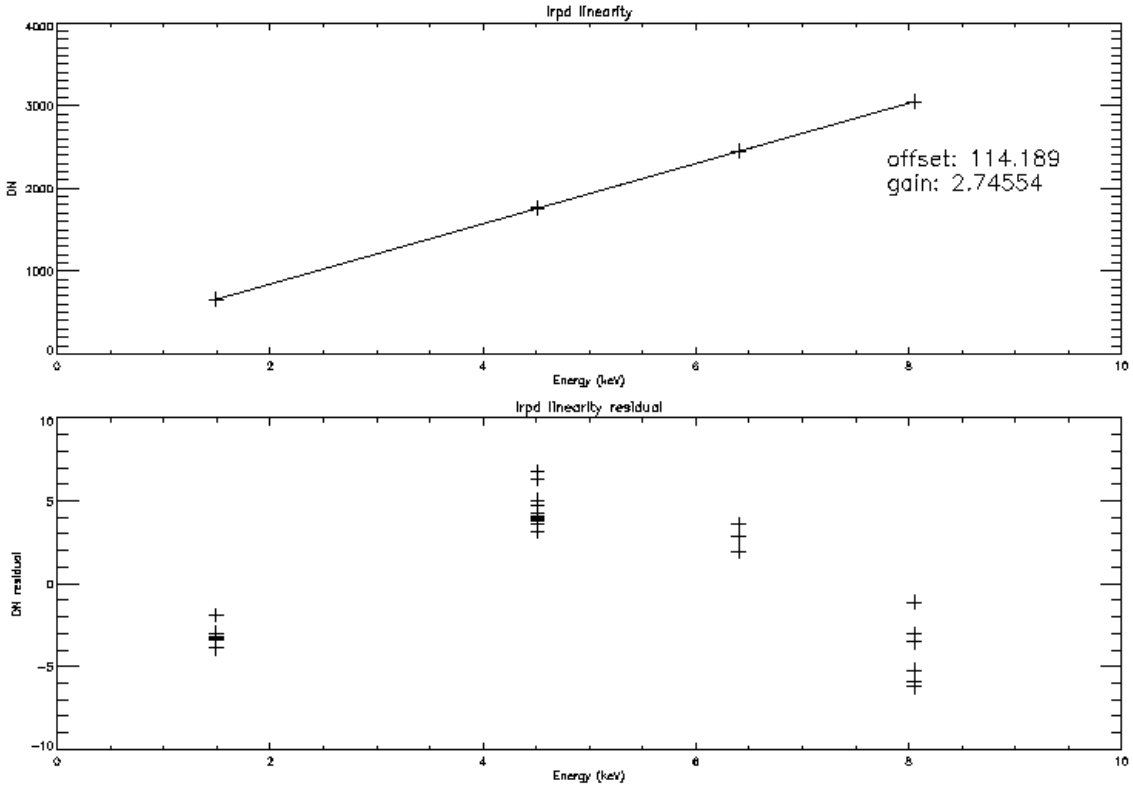

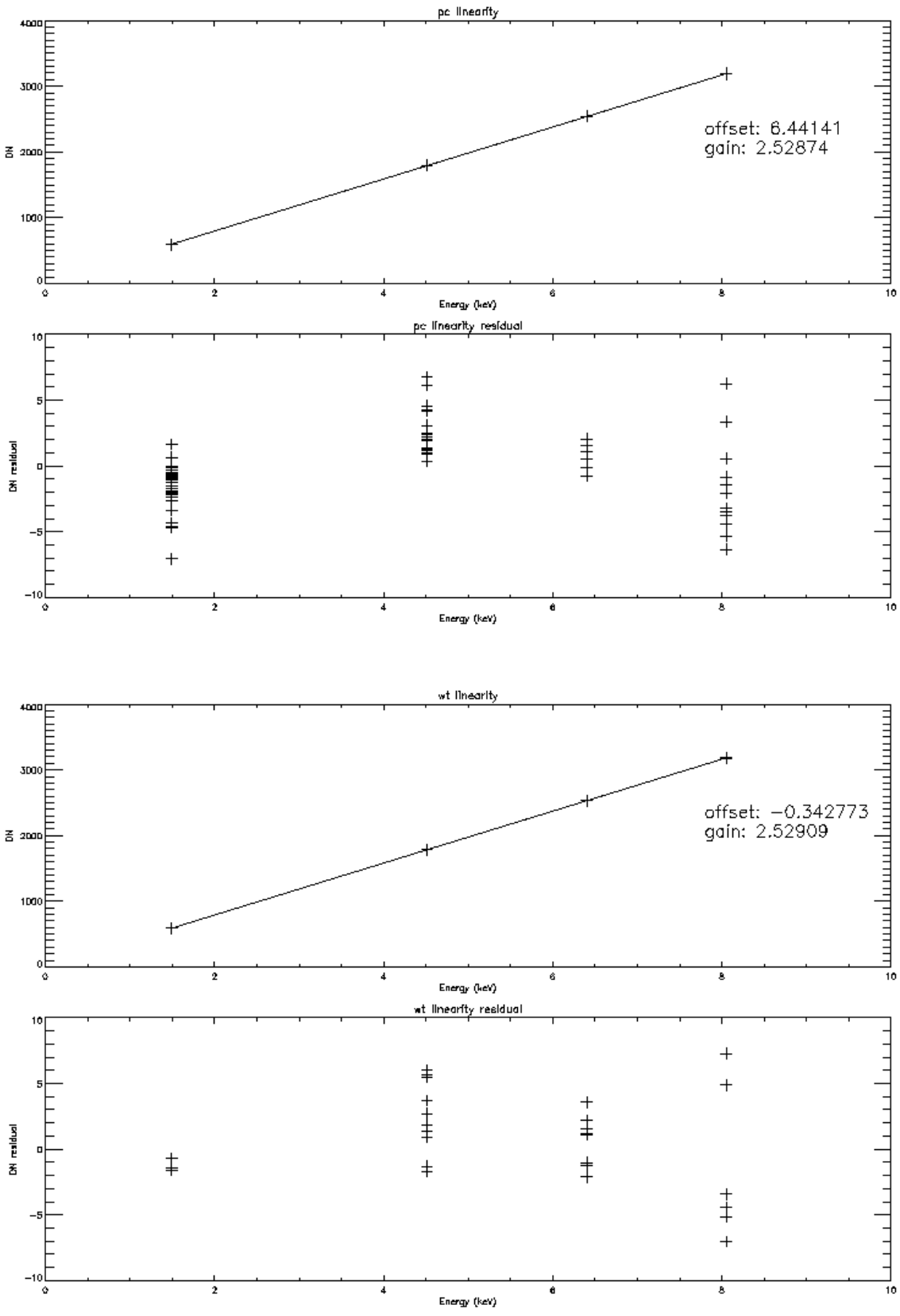

Fig. 8: Gain linearity for the different XRT readout modes.

Thermal Vacuum Gain Calibration (LrPD):

One amendment to the above strategy has become necessary because the low-rate photodiode mode (LrPD) waveform was altered after the completion of the Panter calibration period, changing the value of the nominal gain for this mode. To recalibrate the LrPD mode gain, we have performed a linear fit to the Mn Kα (5.895 keV doublet) and Mn Kβ (6.490 keV) lines collected in thermal vacuum testing during June 2004 (after the waveform change, with CCD temperature of –100 C). The nominal gain values determined as described above for each mode are:

low rate photodiode: 2.55 eV/DN
photon counting: 2.529 eV/DN
windowed timing: 2.529 eV/DN

Pre-Launch CTI analysis

The CTI analysis is performed using Mn Kα data from the thermal vacuum testing period (with CCD temperature of –100 C). Approximately 1.9×10^6 single pixel events have been selected from the output of the PSU *pass1* software from the following list of days/observations:

150_0355	150_0448	150_0719	150_1050
152_1658	153_0234	155_0351	158_1031
159_1935	160_0403	160_0500	160_0816
160_1956	160_2153	160_2327	161_0146

These events are composed both of corner source events (about 1×10^5 events) and door source events (about 1.8×10^6 events).
The initial strategy for determining the global CTI coefficients for the detector is to measure the Gaussian centroid of the Mn k-α events from each of the 4 corner sources, where we have defined a 50 pixel x 50 pixel square region at each corner of the detector to spatially select events. We then calculate the difference in the Gaussian centroids measured at CS1 and CS2 divided by the mean Detector X position as the fractional serial CTI coefficient (that is, the calibration file CTI coefficient times the photon DN value). The parallel CTI coefficient is measured analogously using the CS1-CS3 corner source pair and also using the CS2-CS4 pair.

The Gaussian centroids found for each individual corner source are shown below with 1-sigma Gaussian line width (FWHM/2.35) shown in parentheses and estimated errors:

CS1: 2326.2 +/- 1 (22.8 +/- 1) DN
CS2: 2322.5 +/- 1 (23.7 +/- 1) DN
CS3: 2328.7 +/- 1 (22.5 +/- 1) DN
CS4: 2324.3 +/- 1 (23.1 +/- 1) DN

Using the strategy outlined above, these Gaussian centroid values lead to serial and parallel CTI measures of (errors estimated):

2-4 parallel: 2.0x10-6 +/- 2x10-6
1-3 parallel: 1.4x10-6 +/- 2x10-6
3-4 serial: 3.4x10-6 +/- 2x10-6

Using the door source counts, though, we can investigate the parallel CTI in greater detail by actually mapping out the parallel CTI column by column. We do so as follows: between columns 50 and 550 (roughly where the door source counts strike the CCD) each column of the detector receives about 3500 counts, evenly distributed among the 600 pixels in the column. Below column 50 and above column 550 where primarily corner source counts reach the detector, we have only about 1000 counts per column. We do a simple least squares linear fit to all the events in each column (one column at a time).

We expect the CTI coefficient found for each individual column using this method to be similar to the coefficients noted above found using only the corner sources, with possible exceptions due to traps in individual columns. The overall average of the CTI coefficients found for each column using this method (average of 596 individual columns since the use of single pixel events excludes columns 1-2 and columns 599-600 from this analysis) is 1.6×10^{-6}, in good agreement with the average value found from the 2 parallel pairs of corner sources of 1.7×10^{-6} (average of 1.4×10^{-6} and 2.0×10^{-6}).

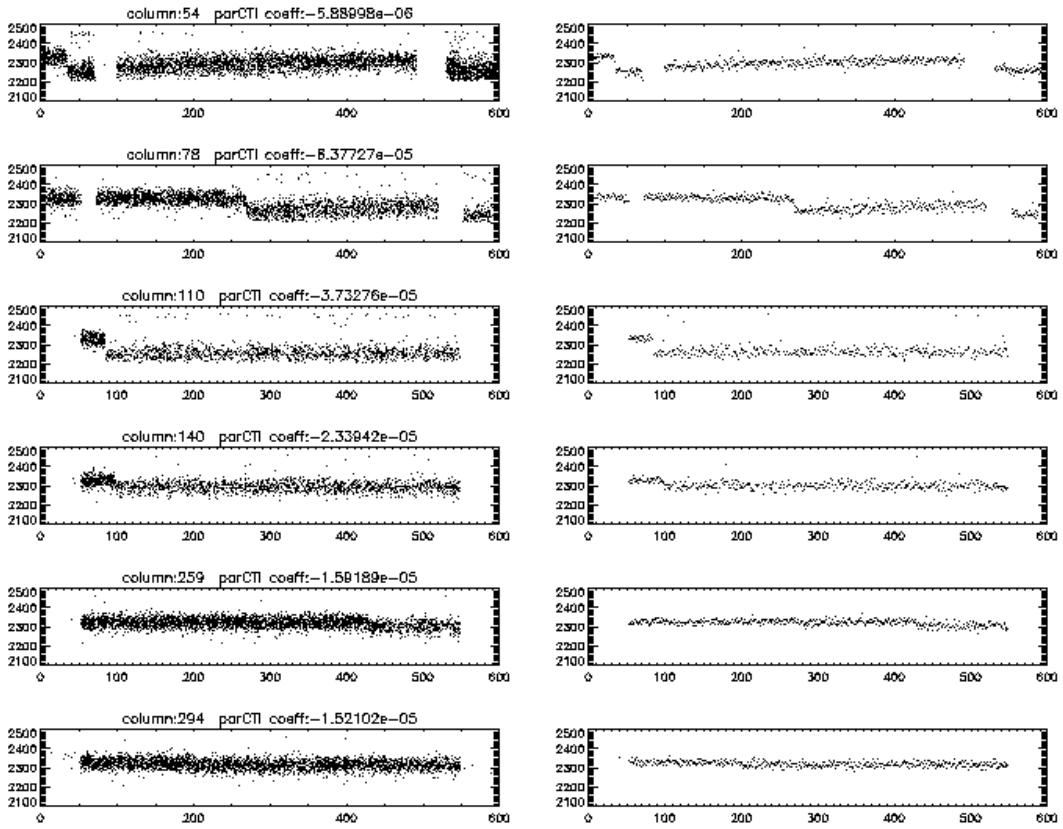

Fig 9: CCD columns presenting charge traps.

We additionally note, however, that there are 6 columns containing significant charge traps; Detector X coord columns: 54, 78, 110, 140, 259, 294. The traps found in columns are demonstrated above in plots of (DN vs row) for each column considered to contain a charge trap. The left plot in each pair shows all events in the column plotted as individual points while the right plot show only the median DN value recorded in each (row) pixel of the column. The top of the left plot in each pair is labeled with the Detector X position column number and the derived parallel CTI coefficient for that column. If we exclude these 6 columns from the average of all column CTI coefficients we did earlier, we find an overall parallel CTI average coefficient of 1.4×10^{-6}, now using 590 columns rather than 596 as before.

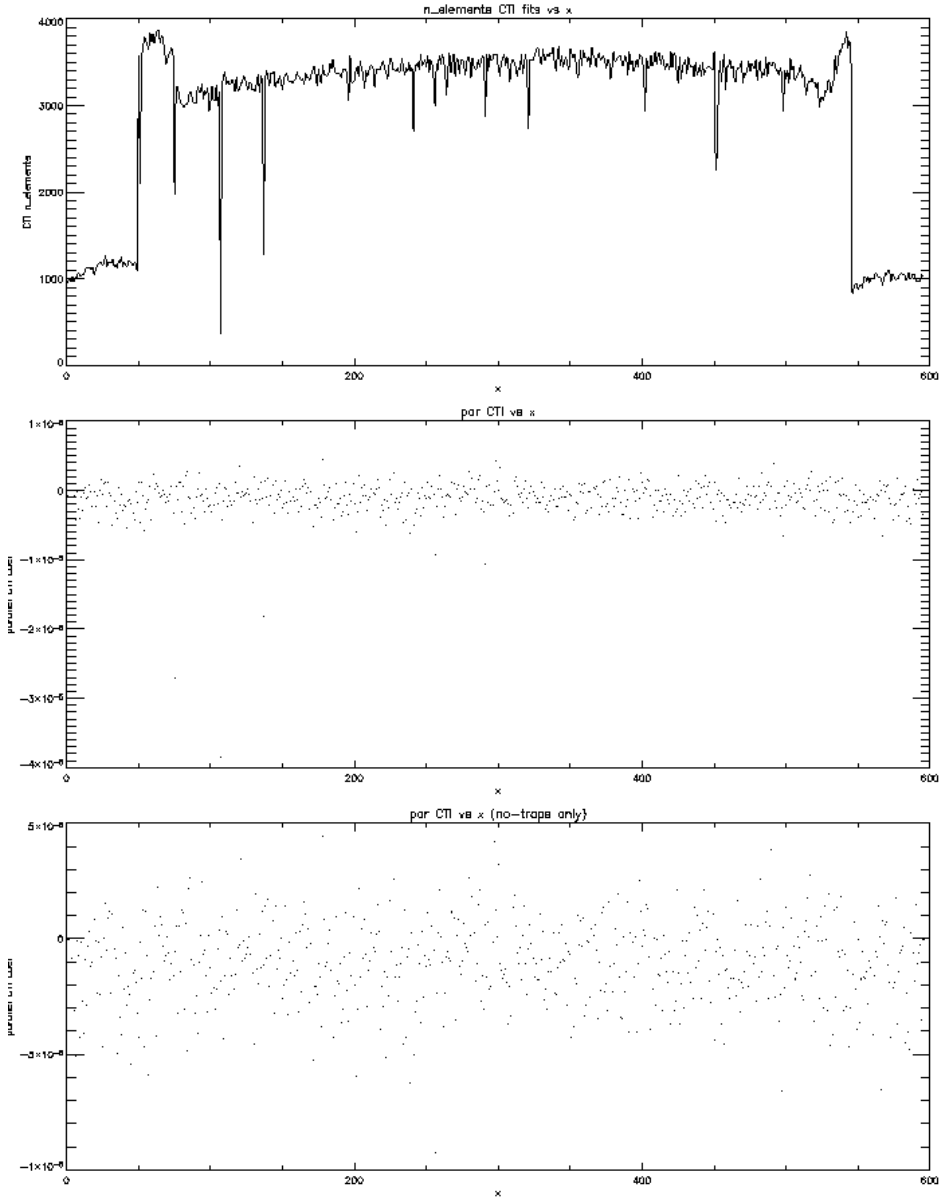

Fig. 10: From top to bottom:

1. number of events vs column number showing that most columns are fit using more than 3000 events and that

no column is fit using fewer than 1000 events

2. plot of the parallel CTI coefficient determined from the individual column fits vs column number. 5 of the 6 columns containing charge traps are clearly identifiable in the figure by the CTI coefficient below $-1x10^{-5}$ while the 6th trapped column (column 54) oddly fits best to a moderate CTI value of $-6x10^{-6}$, though a trap clearly exists (from the plot of DN vs column)
3. expanded view of the CTI coefficient vs column number, where we have shown only the columns believed to not contain a trap.

Given this analysis, we have uploaded gain calibration files (Cal Version 003) to the SDC using the following CTI coefficients:

serial CTI: $3.4x10^{-6}$
parallel CTI: $1.4x10^{-6}$ (the average across the detector)

REFERENCES

1. O. Godet *et al*., "The in-flight spectroscopic performance of the Swift XRT CCD camera during 2006-2007", Proc SPIE 2007, arXiv:0708.2988